Erosion in the tube entrance region of a shell and tube heat exchanger

M.A. Habib, R. Ben-Mansour, H.M. Badr and S.A.M. Said
Mechanical Engineering Department, King Fahd University of Petroleum and Minerals, Dhahran, Saudi Arabia
S.S. Al-Anizi
Saudi Aramco, Dhahran, Saudi Arabia

Received June 2003
Revised January 2004
Accepted February 2004

Abstract

Purpose – In oil and gas industries, the presence of sand particles in produced oil and natural gas represents a major concern because of the associated erosive wear occurring in various flow passages. Erosion in the tube entrance region of a typical shell and tube heat exchanger is numerically predicted.

Design/methodology/approach – The erosion rates are obtained for different flow rates and particle sizes assuming low particle concentration. The erosion prediction is based on using a mathematical model for simulating the fluid velocity field and another model for simulating the motion of solid particles. The fluid velocity (continuous phase) model is based on the solution of the time-averaged governing equations of 3D turbulent flow while the particle-tracking model is based on the solution of the governing equation of each particle motion taking into consideration the viscous and gravity forces as well as the effect of particle rebound behavior.

Findings – The results show that the location and number of eroded tubes depend mainly on the particle size and velocity magnitude at the header inlet. The rate of erosion depends exponentially on the velocity. The particle size shows negligible effect on the erosion rate at high velocity values and the large-size particles show less erosion rates compared to the small-size particles at low values of inlet flow velocities.

Originality/value – In oil and gas industries, the presence of sand particles in produced oil and natural gas represents a major concern because of the associated erosive wear occurring in various flow passages. The results indicate that erosion in shell and tube heat exchanger can be minimized through the control of velocity inlet to the header.

Keywords Erosion, Heat exchangers, Shell structures, Liquid flow

Paper type Research paper

Nomenclature

b	= constant defined in equation (11)	G_k	= generation of turbulent kinetic energy
C_D	= drag coefficient	g	= gravitational acceleration
C_μ	= constant defined in equation (4)	k	= turbulent kinetic energy
C_1	= constant defined in equation (6)	m_p	= mass of individual particle
C_2	= constant defined in equation (6)	p	= pressure
d	= diameter	Re_p	= particle Reynolds number
F	= force		

The support of King Fahd University for this research work is acknowledged.

International Journal for Numerical Methods in Heat & Fluid Flow
Vol. 15 No. 2, 2005
pp. 143-160

0961-5539
DOI 10.1108/09615530510578429

$\overline{U}_j$ = average velocity component
u = fluid velocity vector
$\overline{u}_j$ = fluctuating velocity component
u_p = particle velocity
x_j = space coordinate
t = time

Greek letters
ε = dissipation rate of turbulent kinetic energy
μ = dynamic viscosity
ρ = density
σ_k = effective Prandtl number for k
σ_ε = effective Prandtl number for ε

Superscripts
$-$ = time average

Subscripts
D = drag
f = fluid
sl = Saffman lift
p = particle
pg = pressure gradient
vm = virtual mass

1. Introduction

Erosion is one of the major problems in many industrial processes, as for example, heat exchangers utilizing seawater for cooling purposes and oil and gas production facilities. It results in severe damage of different flow passages causing frequent failure of various equipments and leading to higher cost of maintenance as well as the loss of valuable production time. Solid particle erosion is defined as the loss of material due to repeated application of mechanical forces resulting from the impingement of solid particles on a surface. It is known that sand particle erosion depends on fluid properties, flow structure, sand rate, sand size and the type of metal. The erosion mechanism can occur in the form of direct impingement erosion when the particles have significant momentum toward the walls such as flows in elbows. It can also occur in straight sections such as pipes as a result of turbulent fluctuations that create a mechanism known as random impingement. Erosion may also occur due to the local forces induced by the impingement of liquid droplets on boundary surfaces or due to the very high-localized pressure resulting from cavitation.

The problem of erosion in heat exchanger tubes not only affects the reliability and overall performance of heat exchangers but also increases significantly the cost of operation. The previous work done on erosion in straight tubes, elbows and tees show the strong influence of fluid properties, sand size and flow velocity on the rate of erosion (Rochester and Brunton, 1974; True and Weiner, 1976; Glaeser and Dow, 1977; Roco *et al.*, 1984; Venkatesh, 1986; Shook *et al.*, 1987). The recent experimental study by McLaury *et al.* (1997) on erosion in elbows and straight pipes provided correlations between the penetration rate and the velocity at different elbow diameters and sand rate and size. Edwards *et al.* (2000) reported the effect of the bend angle on the normalized penetration rate. The objective of most of these experimental studies was to provide data for establishing a relationship between the amount of erosion and the physical characteristics of the materials involved, as well as the particle velocity and impact angle.

One of the difficult problems faced in predicting the rate of erosion numerically is the determination of the particle impact velocity, impingement angle and the frequency of surface impacts. The numerical approach to erosion modeling constitutes a combination of flow modeling, Lagrangian particle tracking, and the use of erosion equations. This model, which is sometimes called the Lagrangian approach, requires

expertise in fluid dynamic modeling and a large amount of computational work. In this approach, it is assumed that the particles are not interacting within the flow field. The conditions for this phenomenon correspond to fairly dilute systems characterized by volume fractions (volume of solids/total volume) of less than 10^{-3} (Humphrey, 1990; Keating and Nesic, 2000). While a Lagrangian description of particle motion implies a discrete particle phase, an Eulerian description treats the particle phase as a continuum that permits appropriate definitions of averaged fluid quantities. Many authors carried out comparisons between the Lagrangian and Eulerian approaches, as for example, the work by Durst *et al.* (1984) and Boulet *et al.* (1999). The utilization of computational fluid dynamics (CFD) for obtaining the flow field characteristics together with modeling particle trajectories using Lagrangian simulation of particle motion can predict erosive wear in a complex geometry such as that of multi-orifice choke valves (Wallace *et al.*, 2000).

Graham (1996) summarized the approaches used for developing Lagrangian models in the research conducted prior to 1996. Wang *et al.* (1996) developed a computational model for predicting the rate of erosive wear in a 90° elbow. The flow field was first obtained through a computational model in which the governing equations of motion were solved numerically, thereby neglecting the presence of the solid particles (single-phase flow). The particle trajectory and impacting velocity were then determined by solving the equation of particle motion taking into consideration all forces including drag, buoyancy and virtual mass effects. The penetration rate was then obtained using a semi-empirical relation that was previously developed by Ahlert (1994). A comparison between the predicted penetration rates and the available experimental data showed a good agreement. The investigation also showed that long-radius elbows yielded a lower penetration rate in comparison with the short-radius elbows. However, the results obtained are only valid for 90° elbows and for the two cases of sand particles in air and in water.

McLaury *et al.* (1997) extended the mechanistic model that was developed earlier for predicting erosion in standard elbows (Shirazi *et al.*, 1995a, b) to predict erosion in long-radius elbows. In that work, they accounted for the elbow radius of curvature and for the effect of turbulent fluctuations of the flow. Their results agreed well with the experimental data and the results obtained using a general model consisting of a flow model, a particle-tracking model, and an erosion model. They also developed a mechanistic model for predicting erosion in straight pipes. In that model, random impingements were employed in the erosion mechanism to predict penetration rates. The prediction of penetration rates in long radius elbows and in straight pipes was carried out using semi-empirical correlations. The results for air and water showed a good agreement with those obtained using a general model. More recently, other Lagrangian models involving the use of CFD packages were developed, as for example, the use of PHOENICS by Keating and Nesic (2000) and Hanson and Patel (2000). In addition, the CFX code was used by Forder *et al.* (1998) for predicting erosion within oilfield control valves and the CFD code was used by Edwards *et al.* (2000) to predict erosion in a pipe bend fitting made of carbon steel.

Although the tube entrance region in heat exchangers is the most critical with respect to erosion, there is no research published in the literature that deals with the effect of various parameters on erosion in that region. The present research work aims at studying the effect of different fluid flow parameters on the rate of erosion at the

entrance region of heat exchanger tubes under conditions simulating the normal working conditions of a typical shell and tube heat exchanger. The calculations of flow patterns and solid particle trajectories inside the inlet header of the heat exchanger were performed and the correlations available in the literature were used for estimating the rate of erosion.

2. The flow domain and the governing parameters

The calculations were performed inside the inlet header of the heat exchanger and the tubes of the sheet tube. The tube material is carbon steel. Figure 1 shows the geometry of the header. Flow of water (having density of 998.2 kg/m^3, specific heat of 4,182 J/kg K and laminar viscosity of 0.001003 kg/ms) enters the nozzle of the heat exchanger header. Abrupt expansion occurs at connection with the header. Water then flows toward the tube sheet. The tube sheet has 824 tubes of diameter 14.83 mm distributed in half a cycle as shown in the figure. Owing to symmetry, only half of the tubes were considered. Top hat profile of inlet flow velocity was considered at the header inlet section (Figure 1). The flow velocity ranged from 0.1 to 2.6 m/s. Sand particles of density 2,650 kg/m^3 having diameter in the range 10-350 μm were considered. The number of injected particles is 400.

3. The calculation procedure

It has been established that the rate of erosion in tubes depends upon many parameters such as the properties of the impacting particles, the properties of the tube material, and other parameters of the impact process (Tilly, 1979; Ruff and Wiederhorn, 1979; Davies *et al.*, 1991). Thus, the flow field characteristics and the details of the particle impact process as well as the erosion rate correlations are required for the prediction of the rate of erosion in tubes. In the present work, the Lagrangian particle tracking method is used to model the erosion process and is normally carried out utilizing the following steps (Wallace *et al.*, 2000):

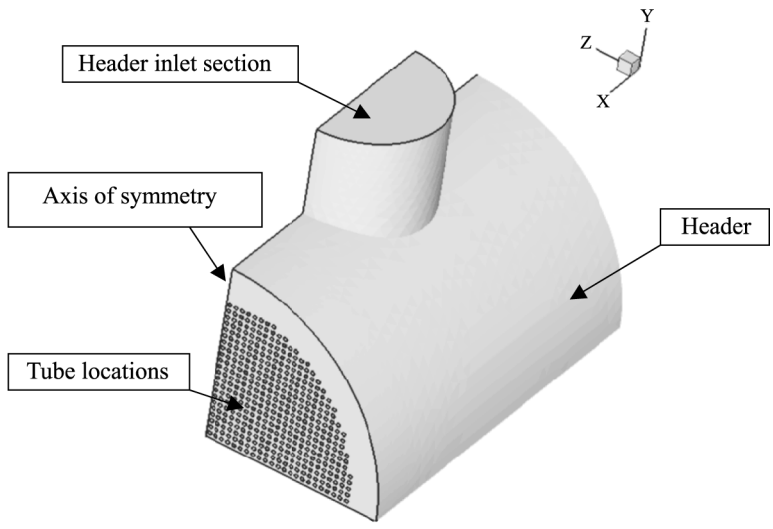

Figure 1.
View of the heat exchanger header

- predict the flow velocity field in the domain of interest;
- calculate the trajectories of solid particles entrained in the fluid using Lagrangian particle tracking calculations and then extract the particle impact data; and
- predict the erosive wear using semi-empirical equations.

The Lagrangian particle tracking method represents a one-way flow-to-particle coupling method that can be used when low volume of particles is simulated. Two computational models were developed. The first is the continuous phase model (dealing with the prediction of the flow velocity field) and the second is the particle-tracking model (dealing with the prediction of particle motion). A brief discussion of the two models is presented in the following sections.

3.1 The continuous phase model

A combination of CFD and Lagrangian particle tracking are normally used to predict the particle movement through complex geometries (Wang *et al.*, 1996; Keating and Nesic, 2000; Edwards *et al.*, 2000; Wallace *et al.*, 2000). To predict the flow pattern of the continuous flow phase, the conservation equations for mass and momentum are solved. Additional transport equations for the turbulence model are also solved since the flow is turbulent. The time-averaged governing equations of 3D turbulent flow can be found in many references (Habib*et al.*, 1989; Versteeg and Malalasekera, 1995) and can be presented as follows.

3.1.1 The continuity and momentum equations.

Mass conservation. The steady-state time-averaged equation for conservation of mass can be written as:

$$\frac{\partial}{\partial x_j}(\rho \overline{U}_j) = 0 \tag{1}$$

Momentum conservation. The steady-state time-averaged equation for the conservation of momentum in the j direction can be expressed as

$$\frac{\partial}{\partial x_j}(\rho \overline{U}_i \overline{U}_j) = -\frac{\partial p}{\partial x_i} + \frac{\partial}{\partial x_j}\left(\mu \frac{\partial U_i}{\partial x_j}\right) - \frac{\partial}{\partial x_j}(\rho \overline{u_i u_j}) \tag{2}$$

where p is the static pressure. The stress tensor $\rho \overline{u_i u_j}$ is given by

$$-\rho \overline{u_i u_j} = \left[\mu_{\text{eff}}\left(\frac{\partial \overline{U}_i}{\partial x_j} + \frac{\partial \overline{U}_j}{\partial x_j}\right)\right] - \frac{2}{3}\rho k \delta_{ij} \tag{3}$$

where δ_{ij} is the Kronecker delta which is equal to 1 for $i = j$ and equals 0 for $i \neq j$ and $\mu_{\text{eff}} = \mu_{\text{t}} + \mu$ is the effective viscosity. The turbulent viscosity, μ_{t}, is calculated using the high-Reynolds number form as

$$\mu_{\text{t}} = \rho C_\mu \frac{k^2}{\varepsilon} \tag{4}$$

where $C_\mu = 0.0845$, k and ε are the kinetic energy of turbulence and its dissipation rate. These are obtained by solving their conservation equations as given below.

3.1.2 Conservation equations for the turbulence model. The conservation equations of the turbulence model (Reynolds, 1987; Shih *et al.*, 1995) are given as follows:

The kinetic energy of turbulence:

$$\frac{\partial}{\partial x_j}(\rho \overline{U}_j k) = \frac{\partial}{\partial x_j}\left(\frac{\mu_{\text{eff}}}{\sigma_k}\frac{\partial k}{\partial x_i}\right) + G_{\text{k}} - \rho\varepsilon \tag{5}$$

The rate of dissipation of the kinetic energy of turbulence:

$$\frac{\partial}{\partial x_j}(\rho \overline{U}_j \varepsilon) = \frac{\partial}{\partial x_i}\left(\frac{\mu_{\text{eff}}}{\sigma_\varepsilon}\frac{\partial \varepsilon}{\partial x_i}\right) + C_{\varepsilon 1} G_{\text{k}} \frac{\varepsilon}{k} - C_{\varepsilon 2}\rho\frac{\varepsilon^2}{k} \tag{6}$$

where G_{k} represents the generation of turbulent kinetic energy due to the mean velocity gradients and is given by

$$G_{\text{k}} = -\rho\overline{u_i u_j}\frac{\partial \overline{U}_j}{\partial x_i} \tag{7}$$

The quantities σ_k and σ_ε are the effective Prandtl numbers for k and ε, respectively, and $C_{\varepsilon 2}$ is given by Shih *et al.* (1995) as a function of the term k/ε and therefore, the model is responsive to the effects of rapid strain and streamline curvature and is suitable for the present calculations. The model constants $C_{\varepsilon 1}$ and $C_{\varepsilon 2}$ have the values; $C_{\varepsilon 1} = 1.42$ and $C_{\varepsilon 2} = 1.68$.

The wall functions establish the link between the field variables at the near-wall cells and the corresponding quantities at the wall. These are based on the assumptions introduced by Launder and Spalding (1974) and have been most widely used for industrial flow modeling. The details of the wall functions are provided by the law-of-the-wall for the mean velocity as given by Habib*et al.* (1989).

3.1.3 Boundary conditions. The velocity distribution is considered uniform at the header inlet section with the velocity in the direction of the nozzle axis. Kinetic energy and its dissipation rate are assigned through a specified value of $\sqrt{k/\overline{U}^2}$ equal to 0.1 and a length scale, L, equal to the diameter of the header inlet nozzle. The boundary condition applied at the exit section (outlet of the heat exchanger tubes) is that of fully developed flow. At the wall boundaries, all velocity components are set to zero in accordance with the no-slip and impermeability conditions. Kinetic energy of turbulence and its dissipation rate are determined from the equations of the turbulence model.

3.1.4 Solution procedure. The conservation equations are integrated and solved simultaneously over a typical volume that is formed by division of the flow field into a number of control volumes, to yield the solution. Calculations are performed with at least 300,000 elements considering fine elements in the section of the header close to the inlet to heat exchanger tubes. Convergence is considered when the maximum of the summation of the residuals of all the elements for U, V, W and pressure correction equations is less than 0.1 percent. The grid independence tests were performed by increasing the number of control volumes from 260,000 to 380,000 in two steps: 260,000-320,000 and 320,000-380,000. The influence of refining the grid on the continuous-phase velocity field is very negligible and indicates that more mesh refinement will result in negligible changes in the results of the computational model.

3.2 Particle tracking

The particle velocity (magnitude and direction) before every impact either on the header walls or anywhere on the tube sheet is needed for the calculation of solid surface erosion and for the determination of the particle trajectory during its course of motion following impact. The particle impact velocity is obtained by determining the particle trajectory from the moment it enters the inlet header until it leaves the heat exchanger tubes. One of the main assumptions in this study is that the solid particles are not interacting with each other (the particles do not collide and the motion of any particle is not influenced by the presence or motion of neighboring particles). Moreover, the influence of particle motion on the fluid flow field is considered very small and can be neglected. These two assumptions are based on the condition of fairly dilute particle concentration. The same assumptions were made by Benchaita *et al.* (1983), Lu *et al.* (1993), Shirazi *et al.* (1995b), Edwards *et al.* (2000), Keating and Nesic (2000) and Wallace *et al.* (2000) in the solution of similar problems of low particle concentration (less than 2-3 percent by weight).

Taking the main hydrodynamic forces into consideration, the particle equation of motion can be written as

$$\frac{\mathrm{d}\underline{u}_\mathrm{p}}{\mathrm{d}t} = F_\mathrm{D}(\underline{u} - \underline{u}_\mathrm{p}) + \underline{g}(\rho_\mathrm{p} - \rho)/\rho_\mathrm{p} + \underline{F}_\mathrm{vm} + \underline{F}_\mathrm{pg} + \underline{F}_\mathrm{sl} \tag{8}$$

where $F_\mathrm{D}(\underline{u} - \underline{u}_\mathrm{p})$ is the drag force per unit particle mass and $F_\mathrm{D} = 3C_\mathrm{D}\mu\mathrm{Re}_\mathrm{p}/4\rho_\mathrm{p}D_\mathrm{p}^2$, $\underline{g}(\rho_\mathrm{p} - \rho)/\rho_p$ is the buoyancy force term, $\underline{F}_\mathrm{vm}$ is the virtual mass term (force required to accelerate the fluid surrounding the particle), $\underline{F}_\mathrm{pg}$ is the pressure gradient term and $\underline{F}_\mathrm{sl}$ is the Saffman lift force (Saffman, 1965). The Magnus lift force (resulting from particle rotation) and the Basset history force (the force accounting for the flow field unsteadiness) have been neglected. The particle Reynolds number, Re_p, and the drag coefficient, C_D are obtained from

$$\mathrm{Re}_\mathrm{p} = \frac{\rho D_\mathrm{p}|\underline{u}_\mathrm{p} - \underline{u}|}{\mu} \tag{9}$$

$$C_\mathrm{D} = a_1 + \frac{a_2}{\mathrm{Re}_\mathrm{p}} + \frac{a_3}{\mathrm{R}_\mathrm{ep}^2} \tag{10}$$

where the a's are constants given by Morsi and Alexander (1972) for smooth spherical particles over several ranges of Re. Another equation that is frequently used for C_D (Haider and Levenspiel, 1989) is given by

$$C_\mathrm{D} = \frac{24}{\mathrm{Re}_\mathrm{p}}\left(1 + b_1 R_\mathrm{ep}^{b_2}\right) + \frac{b_3\mathrm{Re}_\mathrm{p}}{b_4 + \mathrm{Re}_\mathrm{p}} \tag{11}$$

where $b1$, $b2$, $b3$ and $b4$ are expressed in terms of the surface area of a sphere having the same volume as the particle to the actual surface area of the particle.

In the present case of low particle concentration, the particles motions are considered non-interacting and the dominant force in equation (8) is the drag force (Edwards *et al.*, 2000). Some of the other forces given in equation (8) are of small order of magnitude and can be neglected in this study. The first of these is the virtual mass

term that takes care of the force required to accelerate the fluid surrounding the particle. This term can be expressed as

$$\underline{F}_{\mathrm{vm}} = \frac{1}{2}\frac{\rho}{\rho_{\mathrm{p}}}\frac{\mathrm{d}}{\mathrm{d}t}(\underline{u} - \underline{u}_{\mathrm{p}}) \tag{12}$$

and is important when $\rho > \rho_{\mathrm{p}}$ which is not the case in the present study. The second force is that due to pressure gradient, $\underline{F}_{\mathrm{pg}}$, that arises from the influence of the pressure gradient in the flow which acts on every volume element of the flowing medium and can be written as:

$$\underline{F}_{\mathrm{pg}} = \left(\frac{\rho}{\rho_{\mathrm{p}}}\right)\underline{\nabla} p \tag{13}$$

The above statement implies that the pressure does not vary significantly over a distance of one particle diameter, a condition that is normally satisfied for reasonably small particles. Accordingly, the pressure gradient force is neglected in the present study not only due to the small size of the particles but also due to the small pressure gradient prevailing in the flow field. The other forces include the thermophoretic force which is related to small particles suspended in a gas that has a temperature gradient. The particles under such circumstances experience a force in the direction opposite to that of the gradient. Brownian force (Li and Ahmadi, 1992) applies for sub-micron particles. These forces are neglected in the present study. The Saffman's lift force or lift due to shear is also neglected.

3.2.1 Integration of the particle trajectory equations. The particle trajectory equations are solved by stepwise integration over discrete time steps. Integration in time of the equation of particle motion yields the velocity of the particle at each point along the trajectory, with the trajectory itself predicted by

$$\frac{\mathrm{d}\underline{r}}{\mathrm{d}t} = \underline{u}_{\mathrm{p}}, \tag{14}$$

where $\underline{r}$ is the position vector. The above equation is integrated in each coordinate direction to predict the trajectories of the discrete phase. During the integration, the fluid phase velocity, $\underline{u}$, is taken as the velocity of the continuous phase at the particle position.

3.2.2 Discrete phase boundary conditions. The boundary conditions considered when a particle strikes a boundary surface depends on the nature of that surface and one of the following contingencies may arise.

(1) *Reflection via an elastic or inelastic collision.* Reflection is the term used to describe the particle rebound off the solid boundary with a change in its momentum. The normal coefficient of restitution defines the amount of momentum in the direction normal to the wall that is retained by the particle after colliding with the boundary (Tabakoff and Wakeman, 1982). The coefficient of restitution is taken in the present calculations as 0.9 for the case of reflection at a wall.

(2) *Escape through the boundary.* The calculations of the particle trajectory are terminated at the point when it passes through an open boundary (the exit

section of any of the heat exchanger tubes). When the particle encounters such boundary, it is considered that the particle has escaped and the trajectory calculations are then terminated.

(3) *Trap at the wall.* The trajectory calculations for some particles (normally very few particles) are terminated when the particles get trapped in the flow field. This is found to occur in two cases. The first when a particle circulates in a confined flow zone and the second when a particle is trapped near the base plate of the inlet header where the flow velocity is very small. In such cases, the trajectory calculations are terminated. In the present calculations, 5,000 steps with length scale (step size) of 2 mm were used in integrating the particle equation of motion (equation (8)). This ensured that the number of tracking steps is large enough until all particles leave the domain or it becomes constant. The latter case occurs for particles in low speed recirculation zones.

3.3 The erosion model

The previous experimental results (Davies *et al.* 1991; Isomoto *et al.* 1999) show that the erosive wear-rate exhibits power-law velocity dependence. The velocity exponent ranges from 1.9 to 2.5. The results also indicate that the erosion rate is a function of the angle of impact. It is shown that the influence of the angle of impact depends greatly on the type of material being brittle or ductile. Prediction of erosion in straight pipes, elbows and tees show the strong influence of fluid properties, sand size and flow velocity on the rate of erosion (McLaury and Shirazi, 1998; Shirazi *et al.*, 1995a, b; Postletwaite and Nesic, 1993). Erosion is defined as the wear that occurs when solid particles entrained in a fluid stream strike a surface.

There have been many attempts in the past to represent the solid particle erosion process by an analytical formula that could be used to predict erosion under any condition. The complexity of the erosion process and the number of factors involved has meant that no generally applicable equation has been forthcoming. Almost all of the formulae generated have therefore, some degree of dependence on empirical coefficients provided by various experimental erosion tests. No definitive theory of erosion currently exists, however, a number of qualitative and quantitative models do exist. These are described by Finnie (1958), Finnie *et al.* (1992), Wang *et al.* (1996), Keating and Nesic (2000), Edwards *et al.* (2000) and Shirazi and McLaury (2000).

The empirical erosion equations suggested by Neilson and Gilchrist (1968) were used by Wallace *et al.* (2000) to correlate the experimental erosion data to provide an erosion modeling technique. Wallace *et al.* (2000) provided the following formula that proved to provide good results as compared to the experimental data:

$$E = \left\{ \frac{\frac{1}{2} u_p^2 \cos^2 \alpha \sin 2\alpha}{\gamma} + \frac{\frac{1}{2} u_p^2 \sin^2 \alpha}{\sigma} \right\} \quad \alpha \leq 45^\circ \tag{15}$$

$$E = \left\{ \frac{\frac{1}{2} u_p^2 \cos^2 \alpha}{\gamma} + \frac{\frac{1}{2} u_p^2 \sin^2 \alpha}{\sigma} \right\} \quad \alpha > 45^\circ \tag{16}$$

The material of the heat exchanger tubes is carbon steel similar to that of Wallace *et al.* (2000) and having γ and σ (the cutting wear and deformation wear coefficients) with the values $\gamma = 33316.9$ $\sigma = 77419.7$ for low velocity. These formulae (15) and (16) are used in the present calculations of the erosion rate.

Through the tracking model, impingement information is gathered as particles impinge the walls of the geometry. As particle trajectories are computed, this impingement information is recorded and erosion is computed using the empirical relations. Knowledge of the particle impact speed and impact angle allows the erosion rate to be computed. The ability to predict erosion was provided by the authors through FORTRAN subroutines that are used along with the CFD code.

4. Results and discussion

In order to verify the accuracy of the computational scheme, the problem of erosion in a 4 in. diameter carbon-steel pipe was studied considering flow of water at 140°F at average velocities in the range 1-15 m/s. In this problem, erosion occurs due to the presence of sand particles of diameter 300 μm at a rate of 0.1 ft^3/day similar to the case considered by McLaury *et al.* (1997). The results of the comparison are given in terms of the penetration rate. The penetration rate, p_n, is calculated using the following equation (Wang *et al.*, 1996; Shirazi *et al.*, 1995a):

$$p_n = 31.536 \times 10^6 \frac{\dot{s}}{\rho_m N_p A} E_{lc} \tag{17}$$

where A is the impingement area (m^2), E_{lc} is the local erosion rate (mg/g), N_p is the total number of particles being tracked, p_n is the penetration rate (mm/year), $\dot{s}$ is the sand rate (kg/s) and ρ_m is the density of target material (kg/m^3). Figure 2 shows a comparison between the penetration rates obtained using the present approach and those obtained by McLaury *et al.* (1997) at different flow velocities. The figure indicates reasonable agreement at low flow velocities, however, at high velocities, the deviation

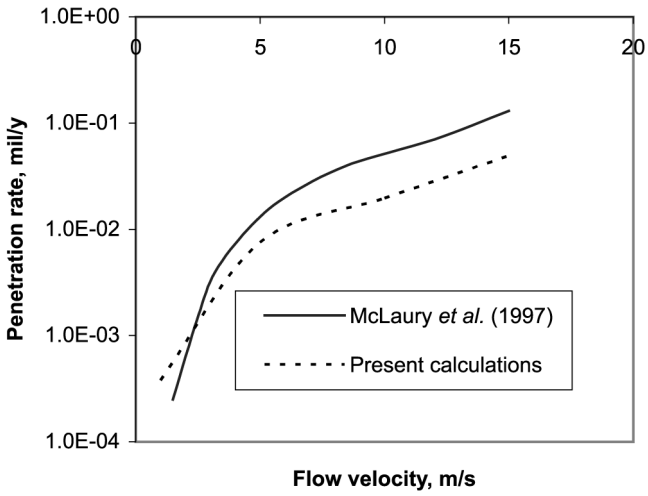

Figure 2.
Comparison between the penetration rate in a 4 in. diameter carbon-steel pipe obtained using the present approach and those obtained by McLaury *et al.* (1997) for the case of water at 140°F and particle diameter of 300 μm

becomes considerable (reaching 60 percent at 15 m/s). It may be noted that the calculations carried out by McLaury *et al.* (1997) incorporated a very simplified model in which a representative particle impact velocity was obtained using a two-dimensional particle tracking across the sublayer and buffer regions. The initial velocity of the particle at the edge of the sublayer was approximated based on the axial flow velocity as well as the turbulent fluctuating velocity at that location. Moreover, the ratio of the number of the particles that impact the tube surface to the amount of the sand flowing in the pipe was estimated via empirical models.

In the present study, erosion rates (mg/g) at the tubes tips of a fixed tube-sheet heat exchanger have been obtained by predicting the fluid flow field at the tube-sheet, calculating the trajectories of particles entrained in the flow field to extract impact data and finally by relating the impact data to erosion wear using the semi-empirical erosion model described above. In calculating the flow field, flow velocity in the range 0.1-2.6 m/s considered. Sand particles of diameter range 10-350 μm were injected at the header inlet section at the same velocity of the flow field.

The study provides in detail the distribution of relative erosion rate at the tip of each tube as well as the total rate of erosion of all tubes and along each line (column) of tubes. The influence of particle size is shown in Figure 3. Figure 3 shows the local erosion rate distribution for three different particle sizes for a header inlet velocity of 0.5 m/s. The figure indicates that the particle size has a large influence on the values of erosion rate and its distribution among the tubes. The small size particles produce severe erosion at low velocities because the scale of eddies produced near the tips of the tubes are too small to involve large size particles. The erosion distribution is affected by the header walls as no erosion was predicted to occur on the tips of a significant number of inner tubes.

The influence of the flow inlet velocity on the erosion rate for a particle size of 200 μm is shown in Figure 4(a)-(d). The figure clearly shows that the rate of erosion increases sharply with increased velocity. The distribution of eroded tubes tips is also greatly influenced by the magnitude of the inlet velocity. This is attributed to the influence of the magnitude of the inlet velocity on the direction and magnitude of the particle impinging velocity at the tube surface. It is also indicated that the number of eroded tubes is increased with the inlet velocity magnitude. The figures show clearly that the location of the tubes which has serious erosion depends on the particle size and velocity magnitude at the inlet section of the header.

Figure 5 shows the influence of the inlet flow velocity on the sum of the erosion rate of all the tubes at different particle sizes. The figure shows the significant influence of the inlet velocity. The erosion rate increases exponentially with the inlet velocity. The erosion rate is less influenced by the particle size and this effect is again the function of the inlet velocity and only shows some dependence at the low velocity range. At low velocity, the influence of buoyancy is significant and therefore, the large-size particles show less erosion rates compared to the small-size particles at low values of inlet flow velocities as shown in Figure 5.

As shown in Figure 3, the erosion is not homogeneous among the tubes, therefore, it is essential to plot the erosion rate for each row of tubes to indicate the lines of tubes and the tube which has the serious erosion. Figure 6 shows the influence of the inlet flow velocity on the erosion rate of the tube line that has maximum erosion rate at different particle sizes. The figure confirms the results shown in Figure 5. Figure 7 shows the influence of the inlet flow velocity on the erosion rate of the single tube that

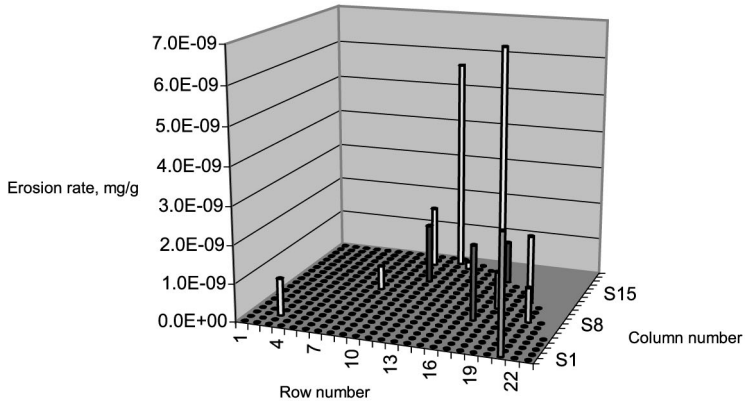

(a) Particle diameter, $d_p = 10$ μm

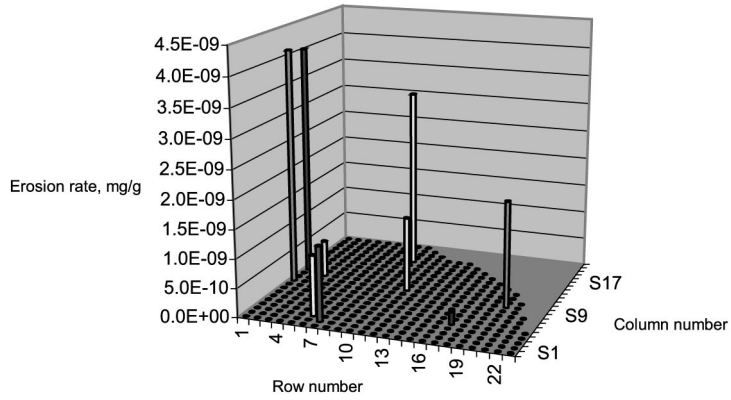

(b) Particle diameter, $d_p = 200$ μm

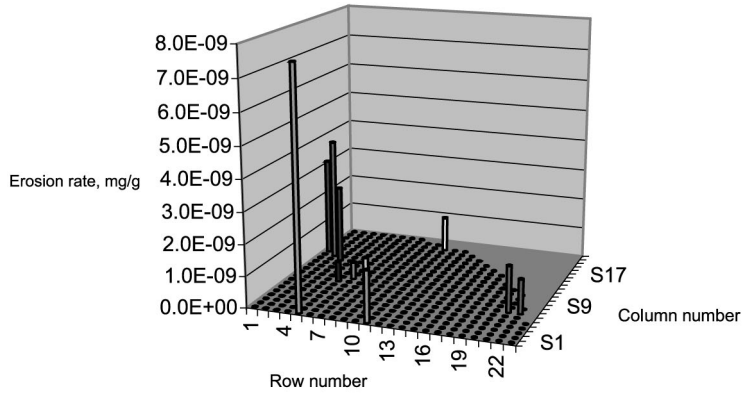

(c) Particle diameter, $d_p = 350$ μm

Figure 3.
The pipe erosion rates for particle diameters of 10, 200 and 350 μm at inlet flow velocity of 0.5 m/s

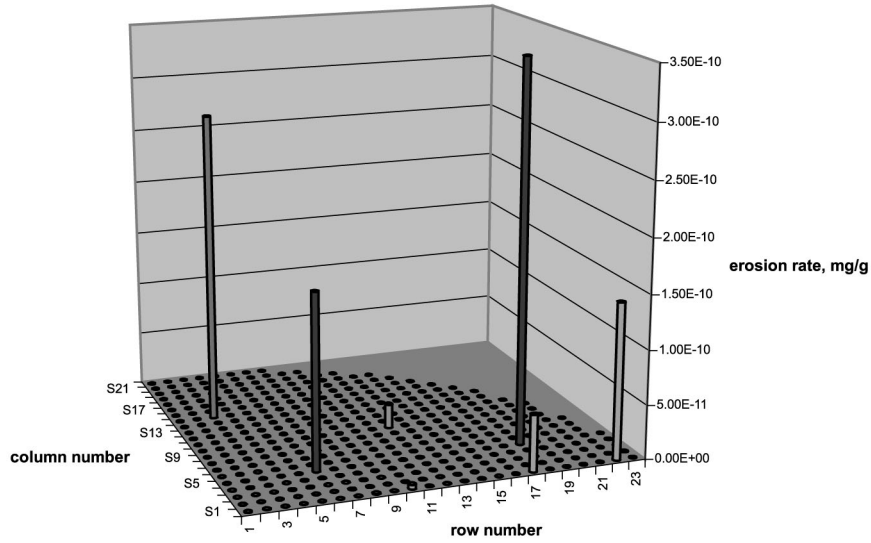

(a) Pipe erosion rate for particle diameter of 200 um at velocity of 0.128 m/s

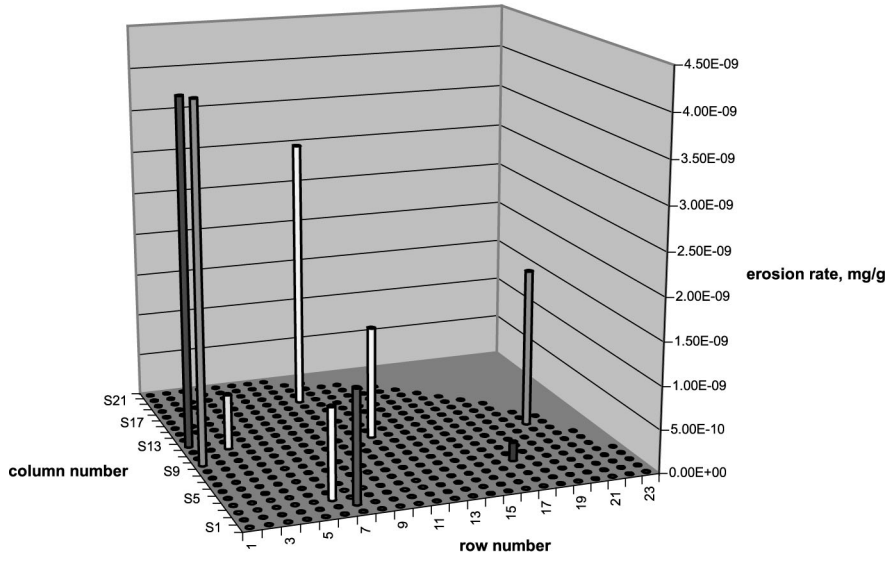

(b) Pipe erosion rate for particle diameter of 200 um at the inlet flow velocity of 0.5 m/s

(Continued)

Figure 4.
Pipe erosion rate for particle diameter of 200 μm at inlet flow velocity of: (a) 0.128 m/s; (b) 0.5 m/s; (c) 1.024 m/s; and (d) 2.56 m/s

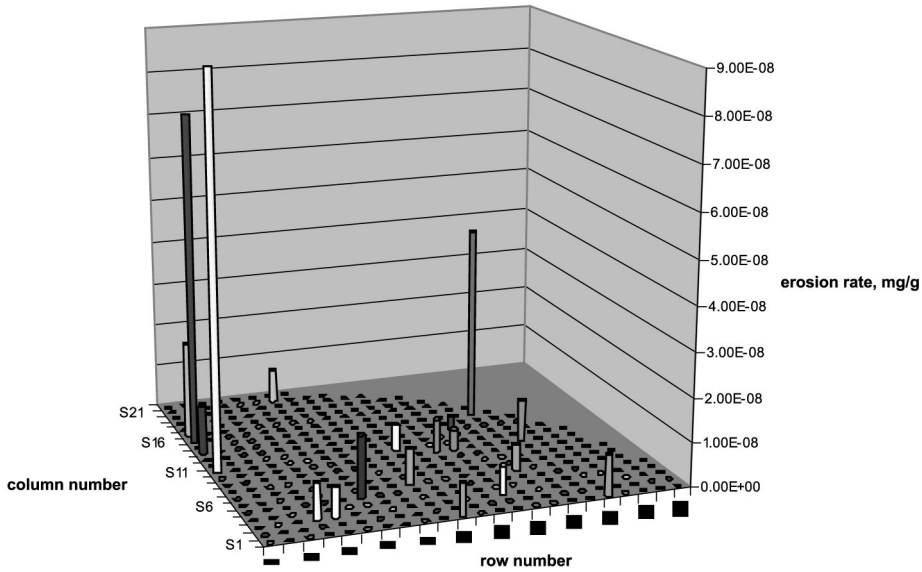

(c) Pipe erosion rate for particle diameter of 200 um at inlet flow velocity of 1.024 m/s

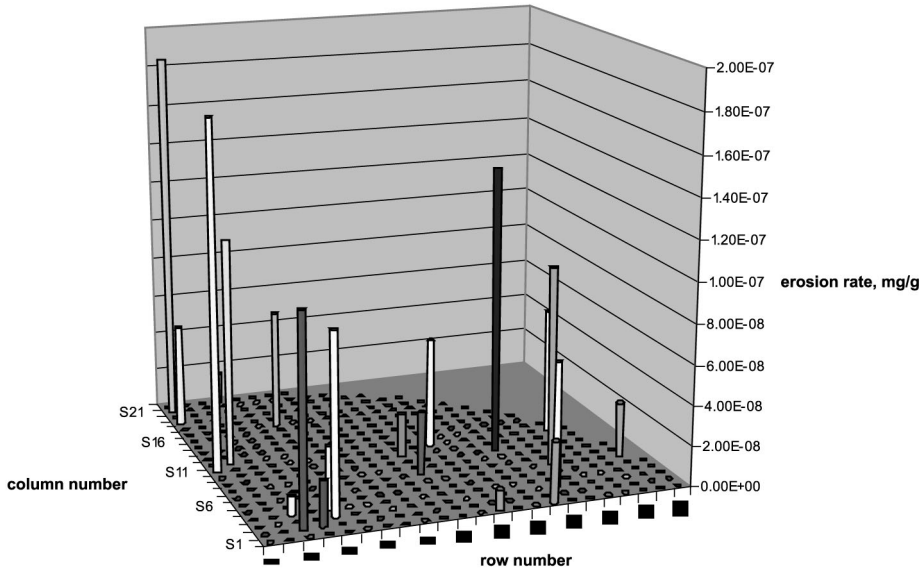

(d) Pipe erosion rate for particle diameter of 200 um at inlet flow velocity 2.56 m/s

Figure 4.

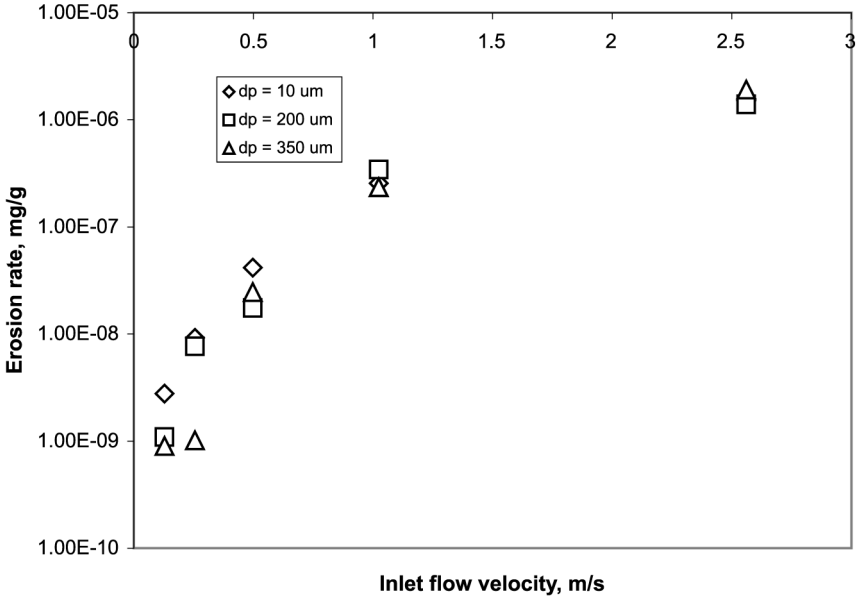

Figure 5.
Influence of inlet flow velocity on total erosion rate

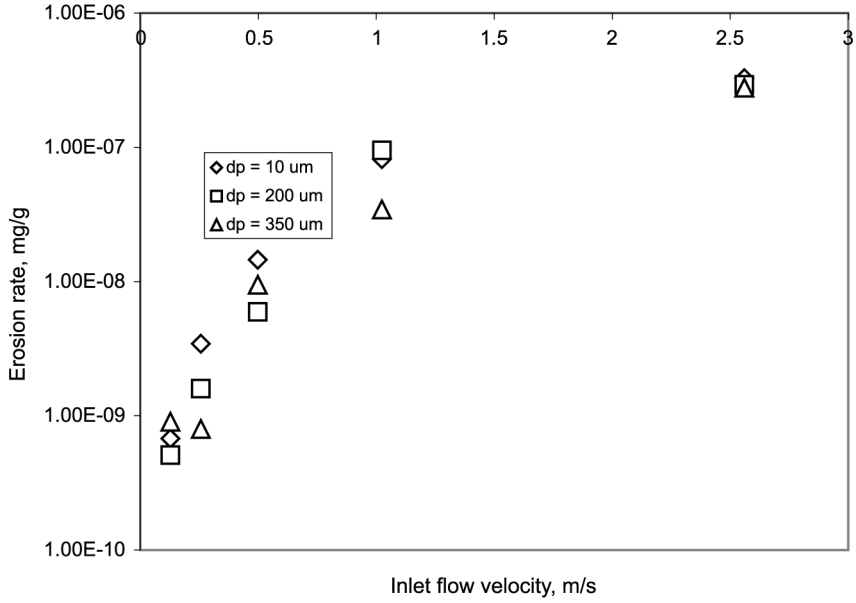

Figure 6.
Influence of the inlet flow velocity on maximum erosion rate over a tube line

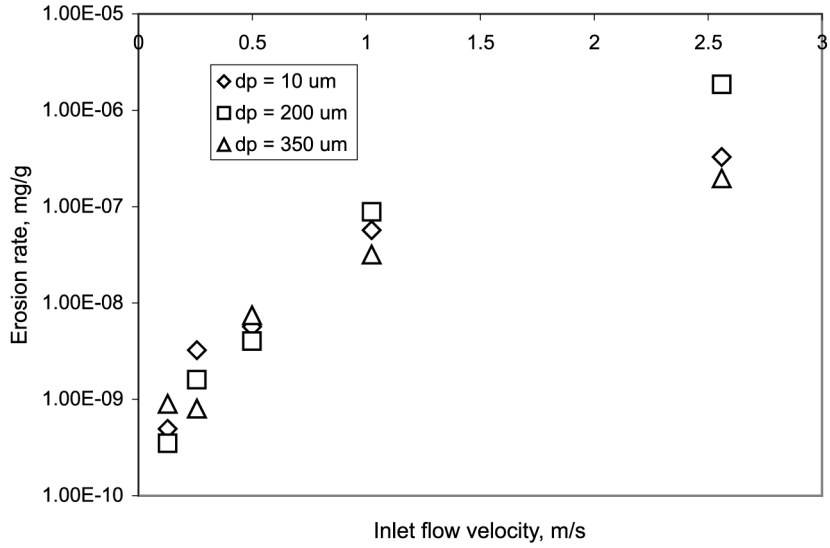

Figure 7.
Influence of the inlet flow velocity on maximum erosion rate of a tube

has maximum erosion rate at different particle sizes. The figure shows a significance of both the inlet flow velocity and particle size.

5. Concluding remarks

Two mathematical models for the calculations of the flow velocity field and the motion of the solid particles have been established. Inlet flow velocity ranged from 0.1 to 2.6 m/s and the study covered a range of particle diameters of 10-350 μm. The results show that the location and number of eroded tubes depend mainly on the particle size and velocity magnitude at the header inlet. The rate of erosion depends exponentially on the velocity at inlet section of the header. The particle size shows negligible effect on the erosion rate at high velocity values and the large-size particles show less erosion rates compared to the small-size particles at low values of inlet flow velocities.

References

Ahlert, K.R. (1994) "Effects of particle impingiment angle and surface wetting on solid particle erosion on ANSI 1018 steel", MS thesis, University of Tulsa, Tulsa, USA.

Benchaita, M.T., Griffith, P. and Rabinowicz, E. (1983), "Erosion of metalllic plate by solid paticles entrained in a liquid jet", *Journal of Engineering for Industry*, Vol. 105, pp. 215-22.

Boulet, P., Oesterle, B. and Andreux, R. (1999), "Comparisons between Eulerian-Eulerian and Eulerian-Lagrangian formulation of a gas-solid suspension flow in a heated pipe", *Proceedings of the 1999 ASME Fluids Engineering Division Summer Meeting*, San Francisco, CA, FEDSM99-7860.

Davies, J.E., Stead, R.J., Andrews, C.J. and Richards, J.R. (1991), "The airborne particle erosion resistance of a range of engineering materials", *Key Engineering Materials*, Vol. 117, pp. 45-52.

Durst, F., Milojevic, D. and Schonung, B. (1984), "Eulerian and Lagrangian predictions of particulate two-phase flows: a numerical study", *J. Appl. Math. Modeling*, Vol. 8, pp. 101-15.

Edwards, J.K., McLaury, B.S. and Shirazi, S.A. (2000), "Evaluation of alternative pipe bend fittings in erosive service", *Proceedings of 2000 ASME Fluids Engineering Summer Meeting*, Boston, MA, 11-15 June 2000, Paper No. FEDSM2000-11245.

Finnie, I. (1958), "The mechanism of erosion of ductile metals", *Proceedings of 3rd US National Congress of Applied Mechanics*, pp. 527-32.

Finnie, I., Stevick, G.R. and Ridgely, J.R. (1992), "The influence of impingement angle on the erosion of ductile metals by angular abrasive particles", *Wear*, Vol. 152, pp. 91-8.

Forder, A., Thew, M. and Harrison, D. (1998), "A numerical investigation of solid particle erosion experienced within oilfield control valves", *Wear*, Vol. 216, pp. 184-93.

Glaeser, W.A. and Dow, A. (1977), "Mechanisms of erosion in slurry pipelines", *Proceedings of the Second International Conference on Slurry Transportation*, Las Vegas, NV, 2-4 March, pp. 136-40.

Graham, D.I. (1996), "An improved eddy interaction model for numerical simulation of turbulent particle dispersion", *ASME J. Fluids Eng.*, Vol. 118, pp. 819-23.

Habib, M.A., Attya, A.E. and McEligot, D.M. (1989), "Calculation of turbulent flow and heat transfer in channels with streamwise periodic flow", *ASME Journal of Turbomachinery*, Vol. 110, pp. 405-11.

Haider, A. and Levenspiel, O. (1989), "Drag coefficient and terminal velocity of spherical and nonspherical particles", *Powder Technology*, Vol. 58, pp. 63-70.

Hanson, R. and Patel, M.K. (2000), "Development of a model to predict the life of pneumatic conveyor bends subject to erosive wear", *Proceedings of 2000 ASME Fluids Engineering Summer Meeting*, Boston, MA, 11-15 June 2000, Paper No. FEDSM2000-11246.

Humphrey, J.A.C. (1990), "Fundamentals of fluid motion in erosion by solid particle impact", *Int. J. Heat and Fluid Flow*, Vol. 11 No. 3, pp. 170-95.

Isomoto, Y., Nishimura, M., Nagahashi, K. and Matsumura, M. (1999), "Impact angle dependence of erosion by solid particle impact for metallic materials", *Erosion Engineering*, Vol. 48 No. 6, pp. 355-61.

Keating, A. and Nesic, S. (2000), "Particle tracking and erosion prediction in three-dimensional bends", *Proceedings of 2000 ASME Fluids Engineering Summer Meeting*, Boston, MA, 11-15 June 2000, Paper No. FEDSM2000-11249.

Launder, B.E. and Spalding, D.B. (1974), "The numerical computation of turbulent flows", *Computer Methods in Applied Mechanics and Engineering*, Vol. 3, pp. 269-89.

Li, A. and Ahmadi, G. (1992), "Dispersion and deposition of spherical particles from point sources in a turbulent channel flow", *Aerosol Science and Technology*, Vol. 16, pp. 209-26.

Lu, Q.Q., Fontaine, J.R. and Aubertin, G. (1993), "A Lagrangian model for solid particles in turbulent flows", *Int. J. Multiphase Flow*, Vol. 19 No. 2, pp. 347-67.

McLaury, B.S. and Shirazi, S.A. (1998), "A predicting erosion in straight pipes", *Proceedings of the 1998 ASME Fluids Engineering Division*, FEDSM 98-5226, Washington DC, 21-25 June.

McLaury, B.S., Wang, J., Shirazi, S.A., Shadley, J.R. and Rybicki, E.F. (1997), "Solid particle erosion in long radius elbows and straight pipes", Society of Petroleum Engineers, Paper No. SPE 38842, pp. 977-86.

Morsi, S.A. and Alexander, A.J. (1972), "An investigation of particle trajectories in two-phase flow systems", *Journal of Fluid Mechanics*, Vol. 52 No. 2, pp. 193-208.

Neilson, J.H. and Gilchrist, A. (1968), "Erosion by a stream of solid particles", *Wear*, Vol. 11, pp. 111-22.

Postletwaite, J. and Nesic, S. (1993), "Erosion in disturbed liquid/ particle pipe flow; effects of flow geometry and particle surface roughness", *Corrosion*, Vol. 49 No. 10, pp. 850-9.

Reynolds, W.C. (1987), "Fundamentals of turbulence for turbulence modeling and simulation", Lecture Notes for Von Karman Institute, Agard Report No. 755.

Rochester, M.C. and Brunton, J.H. (1974), "Influences of physical properties of the liquid on the erosion of solids", *Erosion, Wear and Interfaces with Corrosion*, ASTM STP 567, American Society of Testing and Materials, pp. 128-51.

Roco, M.C., Nair, P., Addie, G.R. and Dennis, J. (1984), "Erosion of concentrated slurries in turbulent flow", *Journal of Pipelines*, Vol. 4, pp. 213-21.

Ruff, A.W. and Wiederhorn, S.M. (1979), "Erosion by solid particle impact", in Preece, C.M. (Ed.), *Treatise on Materials Science and Tehnology*, Vol. 16, Academic Press, New York, NY, pp. 69-125.

Saffman, P.G. (1965), "The lift on a small sphere in a slow shear flow", *Journal of Fluid Mechanics*, Vol. 22 No. 2, pp. 385-400.

Shih, T.H., Liou, W.W., Shabbir, A. and Zhu, J. (1995), "A new k-ε eddy-viscosity model for high Reynolds number turbulent flows – model development and validation", *Computers and Fluids*, Vol. 24 No. 3, pp. 227-38.

Shirazi, S.A. and McLaury, B.S. (2000), "Erosion modeling of elbows in multiphase flow", *Proceedings of 2000 ASME Fluids Engineering Summer Meeting*, Boston, MA, 11-15 June 2000, Paper No. FEDSM2000-11251.

Shirazi, S.A., Shadley, J.R., McLaury, B.S. and Rybicki, E.F. (1995a), "A procedure to predict solid particle erosion in elbows and tees", *Journal of Pressure Vessel Technology*, Vol. 117, pp. 45-52.

Shirazi, S.A., McClaury, B.S., Shadley, J.R. and Rybicki, E.F. (1995b), "Generalization of the API RP 14E Guideline for erosive services", *Journal of Petroleum Technology (Distinguished Author Series)*, Vol. 47 No. 8, pp. 693-8.

Shook, C.A., Mckibben, M. and Small, M. (1987), "Experimental investigation of some hydrodynamics factors affecting slurry pipeline wall erosion", ASME Paper No. 87-PVP-9.

Tabakoff, W. and Wakeman, T. (1982), "Measured particle rebound characteristics useful for erosion prediction", ASME Paper 82-GT-170.

Tilly, G. (1979), "Erosion caused by impact of solid particles", in Preece, C.M. (Ed.), *Treatise on Materials Science and Technology*, Vol. 13, Academic Press, New York, NY.

True, M.E. and Weiner, P.D. (1976), "A laboratory evaluation of sand erosion of oil and gas well production equipment", paper presented at the Annual API Production Division Meeting, Los Angeles, CA, pp. I-1, I-27.

Venkatesh, E.S. (1986), "Erosion damage in oil and gas wells", paper presented at the Rocky Mountain Regional Meeting of the Society of Petroleum Engineers, Billings, MT, SPE Paper 15183.

Versteeg, H.K. and Malalasekera, W. (1995), *An Introduction to Computational Fluid Dynamics; The Finite Volume Method*, Longman Scientific and Technical, Harlow.

Wallace, M.S., Peters, J.S., Scanlon, T.J., Dempster, W.M., McCulloch, S. and Ogilvie, J.B. (2000), "CFD-based erosion modeling of multi-orifice choke valves", *Proceedings of 2000 ASME Fluids Engineering Summer Meeting*, Boston, MA, 11-15 June 2000, Paper No. FEDSM2000-11244.

Wang, J., Shirazi, S.A., Shadley, J.R. and Rybicki, E.F. (1996), "Application of flow modeling and particle tracking to predict sand erosion rates in 90° elbows", FED-Vol. 236, paper presented at the 1996 ASME Fluids Engineering Division Conference, Vol. 1, pp. 725-34.